PROCEEDINGS OF THE ROYAL SOCIETY B

rspb.royalsocietypublishing.org

Research

Cite this article: Lee J-E, Frankenberg C, van der Tol C, Berry JA, Guanter L, Boyce CK, Fisher JB, Morrow E, Worden JR, Asefi S, Badgley G, Saatchi S. 2013 Forest productivity and water stress in Amazonia: observations from GOSAT chlorophyll fluorescence. Proc R Soc B 280: 20130171.
http://dx.doi.org/10.1098/rspb.2013.0171

Received: 24 January 2013
Accepted: 4 April 2013

Subject Areas:
environmental science

Keywords:
chlorophyll fluorescence, Amazon, water stress, drought

Author for correspondence:
Jung-Eun Lee
e-mail: jung-eun.lee@jpl.nasa.gov

†The authors contributed equally to this study.

Electronic supplementary material is available at http://dx.doi.org/10.1098/rspb.2013.0171 or via http://rspb.royalsocietypublishing.org.

Royal Society Publishing
Informing the science of the future

Forest productivity and water stress in Amazonia: observations from GOSAT chlorophyll fluorescence

Jung-Eun Lee[1,†], Christian Frankenberg[1,†], Christiaan van der Tol[2], Joseph A. Berry[3], Luis Guanter[4], C. Kevin Boyce[5], Joshua B. Fisher[1], Eric Morrow[6], John R. Worden[1], Salvi Asefi[7], Grayson Badgley[1] and Sassan Saatchi[1]

[1]Jet Propulsion Laboratory, California Institute of Technology, Pasadena, CA, USA
[2]Faculty of Geo-Information Science and Earth Observation, University of Twente, Enschede, The Netherlands
[3]Department of Global Ecology, Carnegie Institution of Washington, 260 Panama Street, Stanford, CA 94305, USA
[4]Institute for Space Sciences, Free University of Berlin, Berlin, Germany
[5]Department of Geophysical Sciences, University of Chicago, Chicago, IL, USA
[6]Department of Earth and Planetary Sciences, Harvard University, Cambridge, MA, USA
[7]School of Life Sciences, Arizona State University, Tempe, Arizona, CA, USA

It is unclear to what extent seasonal water stress impacts on plant productivity over Amazonia. Using new Greenhouse gases Observing SATellite (GOSAT) satellite measurements of sun-induced chlorophyll fluorescence, we show that midday fluorescence varies with water availability, both of which decrease in the dry season over Amazonian regions with substantial dry season length, suggesting a parallel decrease in gross primary production (GPP). Using additional SeaWinds Scatterometer onboard QuikSCAT satellite measurements of canopy water content, we found a concomitant decrease in daily storage of canopy water content within branches and leaves during the dry season, supporting our conclusion. A large part ($r^2 = 0.75$) of the variance in observed monthly midday fluorescence from GOSAT is explained by water stress over moderately stressed evergreen forests over Amazonia, which is reproduced by model simulations that include a full physiological representation of photosynthesis and fluorescence. The strong relationship between GOSAT and model fluorescence ($r^2 = 0.79$) was obtained using a fixed leaf area index, indicating that GPP changes are more related to environmental conditions than chlorophyll contents. When the dry season extended to drought in 2010 over Amazonia, midday basin-wide GPP was reduced by 15 per cent compared with 2009.

1. Introduction

The Amazon basin represents more than 50 per cent of tropical rainforest area [1], about half of total terrestrial biomass (120 Pg of C of global 247 Pg C) [2], and also hosts a quarter of global biodiversity [3]. How this system might respond to climate change, such as warming and droughts, has been a recent source of debate [4–8]). Observations show a decrease in dry season precipitation over the southern Amazon [9,10], and many Intergovernmental Panel on Climate Change models predict a drier future southern Amazon [11] and an increased dry season length with warming [12]. Plant transpiration partially controls local temperatures, humidity and precipitation [10], which complicates assessment and prediction of land productivity. The productivity and vulnerability of tropical forest critically depends upon how plants cope with water stress in warmer and drier climates, and the question as to what extent changes of dry season length affect the Amazon ecosystem function and may alter its composition is an active research area [8,13].

Several flux towers located in Amazonia report that net ecosystem exchange (NEE) is often higher in the dry season, evapotranspiration rates are maintained through the dry season by deep-rooted trees [14–16] and remote sensing retrievals show either no decrease or even an increase in leaf area during drier periods

[6,17]. Given reduced cloud cover in the dry season, the increased solar influx, possibly increased greenness and deep-rooted trees not affected by surface soil drying, one might expect gross primary production (GPP) of the Amazon ecosystem to increase with drying. However, dry-season NEE increase over Amazonia is caused more by the respiration decrease with drier surface soil [18,19], and GPP can be lower with same transpiration if vapour pressure deficit (VPD) increases during the dry season [20,21]. Hence, it is not clear whether or not GPP is increasing during the dry season. Also, Saleska *et al*. [18] (and [22] to a lesser degree) focused on the GPP (or greenness) increase from the early dry season to late dry season rather than the difference between wet and dry seasons.

Another perspective is provided by an artificial drought experiment in Amazonia [23], which shows that above-ground net primary production declined by 25 per cent over 2 years—indicating that forest productivity decreases under periods of water stress even though, as in this experimental plot, the forest remains green. Consequently, it has been suggested that greenness indices are not sufficient to capture the dynamic response of plants to varying water status [24].

Here, we use sun-induced chlorophyll fluorescence (SIF) to determine the degree of drought stress over Amazonian forests during the dry season. We also use additional satellite data and model simulations to support the SIF measurements.

2. Brief introduction to chlorophyll fluorescence

Photosynthesis (carbon assimilation or GPP), F_p, can be represented by a light-use efficiency (LUE) parametrization as the following equation:

$$F_p = I \cdot f \cdot \varepsilon_p, \tag{2.1}$$

where I is the incident photosynthetically active photon flux density (PPFD), f is the fractional absorption of the incoming light, and ε_p is the efficiency with which light is used in photosynthesis.

Typically, about 1 per cent of the quanta absorbed by chlorophyll are re-emitted at longer wavelengths as fluorescence. As a first approximation, the flux of emitted SIF (F_s) detected by the satellite sensor can be expressed by an equation that is analogous to the expression for photosynthesis,

$$F_s = I \cdot f \cdot \varepsilon_s, \tag{2.2}$$

where ε_s is analogous to the light-use efficiency in equation (2.1) but takes into account both the yield of fluorescence at the leaf level and fraction of it that is captured by the satellite. These equations can be combined and rearranged to give

$$F_p = F_s \frac{\varepsilon_p}{\varepsilon_s}, \tag{2.3}$$

showing that F_p and F_s will have a linear relationship when variation in ε_p and ε_s are parallel tending to keep the ratio $\varepsilon_p/\varepsilon_s$ constant. In the Soil Canopy Observation of Photochemistry and Energy flux (SCOPE) model, ε_p is calculated using a physiological parametrization [25], and ε_s is simulated based on an empirical calibration as was described in §3*d*.

When plants experience stress, heat dissipation increases, with a subsequent decrease in both photochemistry and fluorescence [26–28]. This process, termed non-photochemical quenching (NPQ), is dominant at the light levels that normally occur during daytime in the crown. Flexas *et al*. [26] provide experimental evidence that NPQ is a function of water stress as well as light intensity.

In a previous study, GOSAT chlorophyll fluorescence intensity aggregated to $4^\circ \times 4^\circ$ exhibited moderate to strong linear correlations ($r^2 = 0.5–0.8$) with GPP estimates from several different types of models [29,30]. While these models require substantial input data to obtain GPP—for example, temperature and the degree of water stress—fluorescence appears to show GPP directly without ancillary data. Modelling activities and field campaigns focused on the remote sensing of chlorophyll fluorescence have been carried out in preparation for the FLuorescence EXplorer (FLEX) mission concept of the European Space Agency and provide fundamental context for this study [31,32]. For example, leaf-scale studies show that physiological effects of drought that lead to a decrease in LUE for photosynthesis are associated with decreases in fluorescence yield [26]. Furthermore, canopy-level measurements of fluorescence during an episode of drought demonstrate that fluorescence declines, whereas normalized difference vegetation index (and presumably light absorption) remains constant [27], confirming that the passive measurements of SIF can be used to track changes in GPP at the canopy scale even when there are no changes in greenness. Additionally, SIF from chlorophyll is directly linked via the fluorescence yield to the flux of absorbed sunlight. Leaf abscission and changes in leaf display can affect the flux of sunlight absorbed by chlorophyll and the intensity of the fluorescent 'glow' (i.e. emission) of the canopy. Thus, GOSAT fluorescence should capture changes in GPP associated with *both* changes in LUE and absorbed sunlight.

3. Data and model

We use: (i) SIF, measured by the Greenhouse gases Observing SATellite (GOSAT), which provides information on the physiological state of the canopy at the time of overpass (approx. 13.00 local time) [29,30,33], (ii) radar backscatter measurements of the SeaWinds Scatterometer onboard QuikSCAT (QSCAT) [34], which gives information on forest canopy water status, (iii) monthly rainfall data from the Tropical Rainfall Measuring Mission (TRMM) that captures the precipitation seasonality, and (iv) vegetation indices, the Enhanced Vegetation Index (EVI) and Leaf Area Index (LAI), all of which provide information on the fractional absorption of sunlight and photosynthetic capacity [35].

We selected and compared three regions that are: (A) continually wet, (B) seasonally dry but evergreen, and (C) strongly seasonal, (A, B and C; figure 1) and aggregated monthly measures of fluorescence, precipitation canopy water and moderate resolution imaging spectroradiometer (MODIS) EVI to this scale (figure 2). More information on the seasonality of TRMM rainfall and dry season length are shown in electronic supplementary material, figures S1 and S2. We examine the response of fluorescence to seasonal changes in water relations in these representative areas.

(a) Fluorescence

The fluorescence signal was measured using high-resolution spectra covering Fraunhofer lines (narrow absorption features in the solar atmospheric spectrum) in the 755–772 nm range.

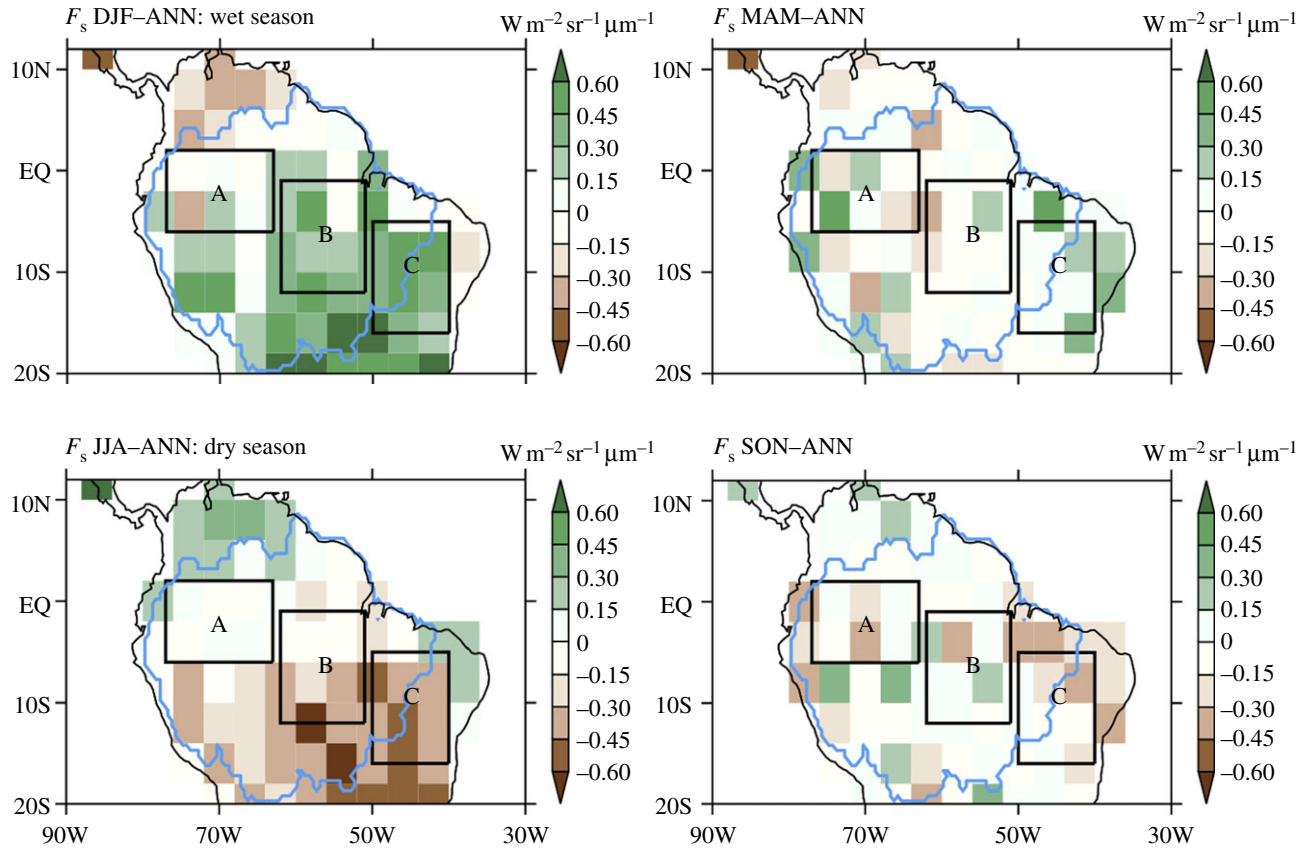

Figure 1. Seasonal variation of chlorophyll fluorescence, F_s (W m^{-2} sr^{-1} µm^{-1}), retrieved from GOSAT in 755 nm over Amazonia during June 2009–May 2010. The annual mean is subtracted from the seasonal mean to show fluorescence seasonality. Boxes A, B and C are relative everwet, wet and dry areas, respectively, for the analysis in figures 2 and 3. The outline in the map line represents the Amazon basin. The resolution in the figure is coarse because GOSAT provides only one measurement at every 4 s and the retrieval exhibits a high single measurement noise. (Online version in colour.)

Spectra were recorded by the thermal and near infrared sensor for carbon observation Fourier Transform Spectrometer (FTS) onboard the Japanese GOSAT satellite, launched on 23 January 2009. The retrieval method, data characterization and post-processing are described in detail in previous publications [29,30]. Each GOSAT retrieval samples a footprint area approximately 10 km in diameter. Averaging in time and space is needed owing to single measurement statistical noise. A typical value for monthly means in this study is $1–1.5 \pm 0.1$ W m^{-2} sr^{-1} µm^{-1}.

A unique and critical step in our data processing is the correction of an observed zero-level offset in acquired GOSAT O_2 A-band spectra, strongly biasing fluorescence because its impact on Fraunhofer line depth is indistinguishable from fluorescence. Compared with the previous analysis, we applied monthly calibration parametrizations for the GOSAT zero-level offset coming from a detector nonlinearity [30]. We overcame this problem by performing calibration steps on a month-to-month basis, allowing for less scatter in fluorescence averages. Fluorescence retrievals are nearly completely unaffected by non-absorbing aerosols [36], unlike vegetation indices based on reflected solar energy that are strongly affected by aerosols [5].

(b) Canopy water content

We chose QSCAT to study the Amazon vegetation water content because: (i) the radar backscatter at microwave frequency (13.4 GHz) and high incidence angle (approx. 46° and 54° from zenith) over dense forest cover are strongly sensitive to the canopy (predominately leaf and branch) water content through the canopy dielectric properties [34,37], and (ii) being an active microwave sensor, QSCAT images over tropical forests have almost no effects from the presence of clouds and aerosols, and no sensitivity to seasonal variations to incoming solar radiation. We used QSCAT backscatter data (σ^0) at H polarization from morning and afternoon passes (6.00 and 18.00 local time) to create monthly estimates of canopy water content by scaling the radar backscatter with the ground measurements of canopy water content for the period of 2009.

(c) MODIS data

The latest version of MODIS land data (Collection 5 product) was used to generate the EVI time series. MOD13A3 data (Vegetation Indices, 1 km resolution, monthly composites) were downloaded from the MODIS Land Processes Distributed Active Archive Center and pre-processed according to the quality assurance filtering criteria described in [5]. MODIS LAI and GPP data are based on the gap-filled version from Zhao & Running [35]. MODIS GPP values are calculated using MODIS greenness indices in conjunction with ancillary meteorological data.

(d) Soil Canopy Observation of Photochemistry and Energy flux (SCOPE) model description

SCOPE [38] is a vertical (one-dimensional) photosynthesis, radiative transfer and energy balance model. Photosynthesis

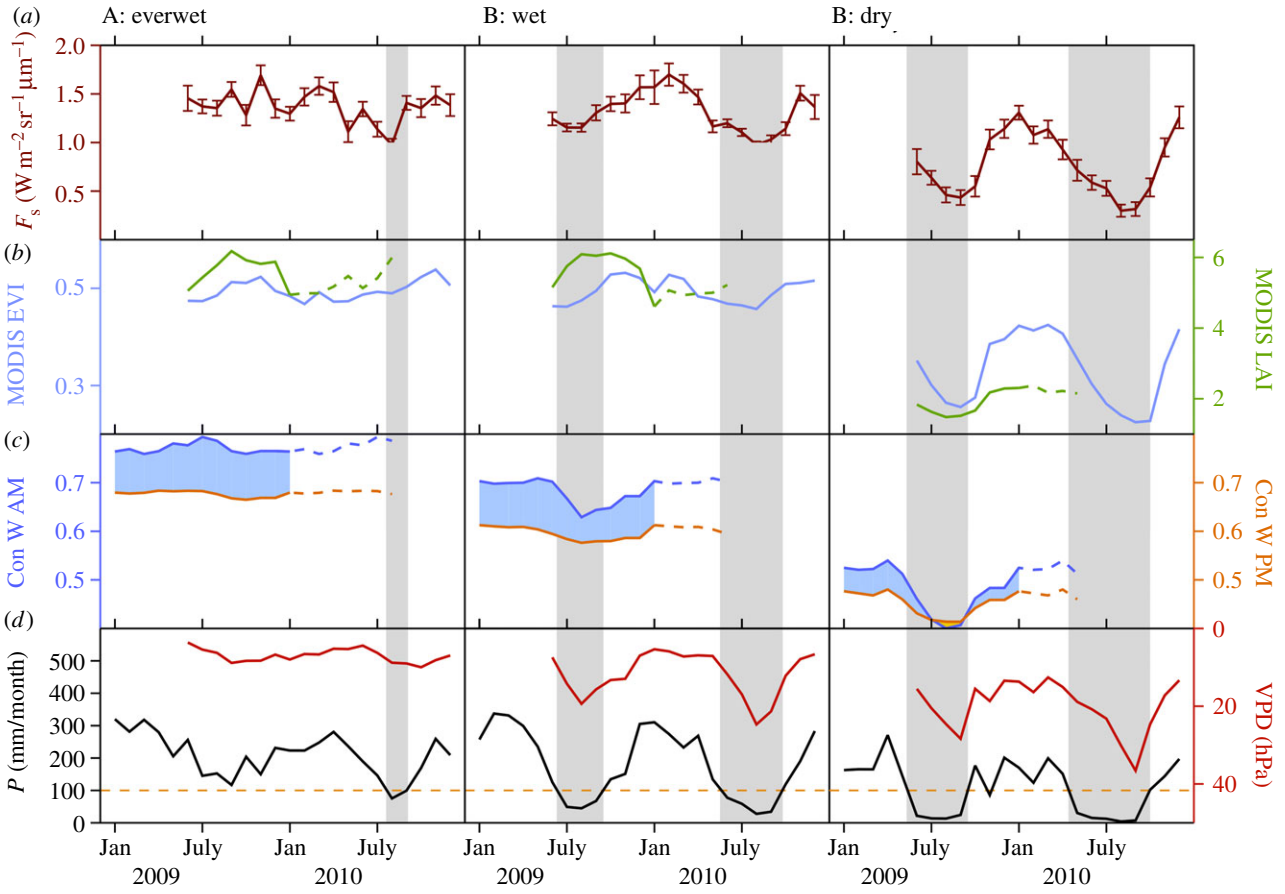

Figure 2. Seasonal variations of fluorescence at 755 nm (W m^{-2} sr^{-1} μm^{-1}) (*a*), and MODIS EVI and LAI (*b*), morning and afternoon canopy water content index from QSCAT (*c*), precipitation (mm day^{-1}) and vapour pressure deficit (VPD; hPa) from European Centre for Medium-Range Weather Forecasts (ECMWF) reanalysis (ERA) at the GOSAT overpass (*d*). Three areas (first column A; second column B; third column C; figure 1) are chosen by considering climatology (length of the dry season) and biome types (see the electronic supplementary material, figure S2). In area A, TRMM climatological precipitation does not drop below 100 mm month^{-1} for all months, area B has three to four months of dry season and area C is outside the rainforest. Gap-filled LAI and canopy water content index are not available for 2010 (2009 values are repeated as dashed lines for illustration). Afternoon canopy water index is higher outside tropical rainforest (region C), implying that plants store water when stomata are closed and plants are taking up water earlier during the day. The error bar in fluorescence indicates the standard error in the monthly average, and the grey area indicates the dry season when mean monthly precipitation is below 100 mm month^{-1}. (Online version in colour.)

is calculated using Farquhar *et al*. [39] and Collatz *et al*. [40] for C3 and C4 plants, respectively. It calculates the illumination of leaves with respect to their position and orientation in the canopy, and the spectra of reflected and emitted radiation as observed above the canopy in (satellite) observation direction. The spectral range (0.4–50 μm) includes the visible, near and shortwave infrared and the thermal domain. The geometry of the vegetation is treated in a stochastic way. We used a canopy structure with a spherical leaf angle distribution with an LAI of six equally distributed over 60 elementary layers. Radiative transfer of chlorophyll fluorescence is calculated using a module similar to the FluorSAIL model [41], but allowing leaf fluorescence to vary depending on position and orientation in the canopy. A leaf-level biochemical model calculates 400–700 nm range fluorescence from the absorbed fluxes, canopy temperature and ambient vapour, CO_2 and O_2 concentrations, in conjunction with GPP, stomatal resistance and the energy balance of the leaf [25]. The model calculates radiation transport in a multilayer canopy as a function of the solar zenith angle and leaf orientation to simulate fluorescence in the observation direction (in this case nadir).

The fluorescence equations in the original SCOPE model were modified to accommodate a decrease in maximum dark-adapted fluorescence, F_m, with increasing stress, following [42]. This was achieved by introducing a rate constant, K_n for additional heat dissipation in case of light adapted conditions on the top of heat dissipation in dark-adapted conditions, K_d. Thus, F_m is formulated in the following:

$$F_m = \frac{K_f}{K_f + K_d + K_n}, \tag{3.1}$$

where K_f is the rate constant for fluorescence. In our formulation, we used 0.05 and 0.95 for K_f and K_d, respectively. Here K_n varies with the balance of excitation and sink strength, suggested by Duysens & Sweers [43]. We calibrated this relation using the empirical data from Galmés *et al*. [28] resulting in

$$K_n = x(6.2473x - 0.5944). \tag{3.2}$$

Here, x $(=1-J_e/J_o)$ is relative reduction of photochemical yield, J_e is the actual electron transport rate calculated from the CO_2 exchange data (the carboxylase limited rate), and J_o is the maximum possible electron transport calculated from the absorbed PPFD and the dark-adapted rate constants.

4. Results

The Amazon basin exhibits substantial spatial and temporal variations in fluorescence (and GPP), and figure 1 depicts

Table 1. Square of correlation coefficient (r) between monthly mean variables. (Correlation coefficient greater than 0.15 is statistically significant at 95% confidence interval. Negative signs in parentheses indicate that the sign of correlation is negative.)

	GOSAT SIF	SCOPE SIF	SCOPE GPP	EVI	VPD
GOSAT SIF	1.00	0.79	0.43	0.52	0.75 (−)
SCOPE SIF	0.79	1.00	0.64	0.29	0.72 (−)
SCOPE GPP	0.43	0.64	1.00	0.01	0.58 (−)
EVI	0.52	0.29	0.01	1.00	0.36 (−)
VPD	0.75 (−)	0.72 (−)	0.58 (−)	0.36 (−)	1.00

the seasonal departures of GOSAT fluorescence from the annual mean on a $4^\circ \times 4^\circ$ grid. Austral summer (December–February) is the relatively wet season, and austral winter (June–August) is the dry season over most of the area south of the equator (see the electronic supplementary material, figures S1 and S2). Dry season length and intensity increases east- and southwards, and the seasonality of fluorescence also increases in those directions.

Over the everwet northwestern Amazonia (region A in figure 1) both fluorescence and MODIS EVI/LAI show small seasonality (figure 2). This contrasts with region C, to the south of the Amazon forest, with deciduous trees and/or grasses (e.g. the cerrado ecosystems), where water stress is more pronounced, and fluorescence and greenness covary with each other. However, over central Amazonia with a relatively moderate dry season of approximately three months (region B), fluorescence decreases significantly (approx. 27%) during the normal (2009) dry season compared with the wet season, while LAI increases by 11 per cent during the dry season. MODIS EVI, on the other hand, shows similar variations to fluorescence ($r^2 = 0.52$). Table 1 summarizes r^2 between different parameters.

As shown in figure 2, canopy water content follows the pattern A > B > C and the diurnal variation in water content tends to be lower during the dry season than in the wet season. Hence, we observe a high negative correlation between VPD and fluorescence ($r^2 = 0.75$ in region B; figure 3*a*), and low fluorescence values during the 2010 drought (filled symbols in figure 3). We point out that VPD is not only a measure of the atmospheric condition, but also is an indicator of soil moisture status and hence water stress as decreased soil moisture limits evapotranspiration, increases temperature and decreases atmospheric moisture content (hence higher VPD).

To provide a more mechanistic basis for analysing the changes in fluorescence and GPP in region B, we performed simulations of GPP and fluorescence using the SCOPE model. The model was run using meteorological data from the European Centre for Medium-Range Weather Forecasts Reanalysis (ERA-Interim) with constant LAI. SCOPE-predicted fluorescence is highly correlated with GOSAT fluorescence ($r^2 = 0.79$; figure 4*a*), and SCOPE-simulated GPP for the Amazon basin was highly correlated with simulated fluorescence ($r^2 = 0.64$; figure 4*b*), as previously observed in a global study [30,31]. Overall, GOSAT fluorescence explains a large part of SCOPE GPP ($r^2 = 0.43$, $p < 0.01$). The correlation between fluorescence and EVI is significant ($r^2 = 0.52$), but EVI is not correlated with SCOPE GPP ($r^2 = 0.01$, figure 4*d*).

During the 'normal' dry season, we observe a 27 per cent in Amazonian fluorescence decline compared with the wet season in midday fluorescence, which is coincident with water stress in soil derived from TRMM rainfall and canopy water observed by QSCAT; this implies a decrease in productivity over a large part of the Amazon forests at midday during the dry season.

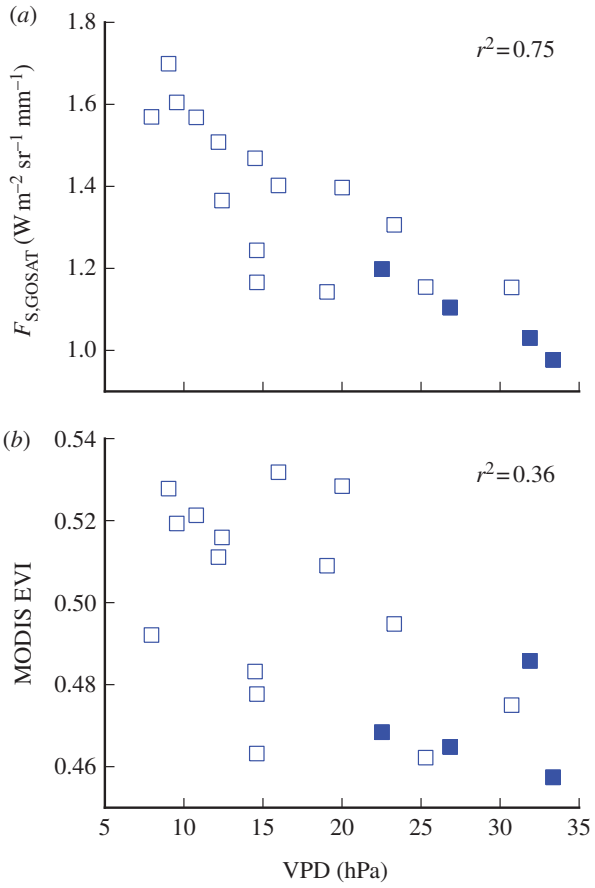

Figure 3. (*a*) The relationship between vapour pressure deficit and GOSAT fluorescence at 755 nm and (*b*) MODIS EVI. Values are monthly mean for region B, and VPD values have been extracted from the ERA dataset at the time and location of the GOSAT measurement. Filled symbols represent values for months with precipitation lower than 100 mm month^{-1} in 2010 during the Amazon drought (June–September). Correlation coefficients are calculated using all values. (Online version in colour.)

5. Discussion

The controversy over whether Amazonian forests are water-limited versus light-limited arose because they maintain high transpiration rate during the dry season and are often

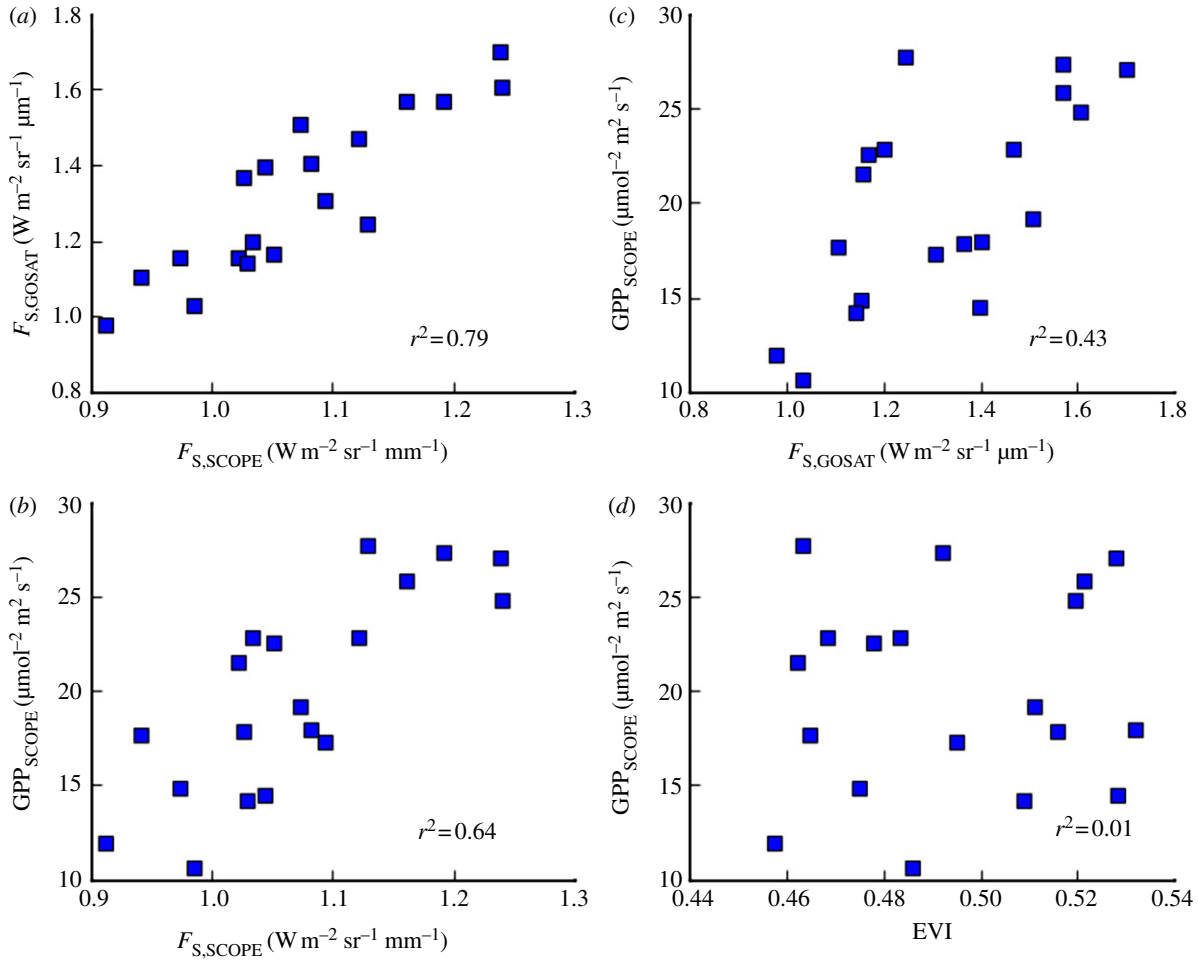

Figure 4. The relationship between steady-state fluorescence at 755 nm (W m^{-2} sr^{-1} μm^{-1}; *x*-axis) from GOSAT and the SCOPE model results (*a*), between SCOPE fluorescence and SCOPE GPP (μmol m^{-2} s^{-1}; *y*-axis) (*b*), and between GOSAT fluorescence and SCOPE GPP for region B. Input meteorology data (insolation, temperature and VPD) are from European Centre for Medium-Range Weather Forecasts (ECMWF). We use a marginal cost of water per unit carbon assimilation, $\lambda = 750$ [49], non-varying leaf area index (LAI) = 6, maximum carboxylation rate, $V_{c,max} = 75$ μmol m^{-2} s^{-1}, and chlorophyll concentration, $C_{ab} = 40$ μg cm^{-2}. All values are over region B and monthly mean values. (Online version in colour.)

covered by clouds during the wet season. Using chlorophyll fluorescence retrieved from GOSAT, we show that while Amazonian rainforests retain high productivity during the dry season as previous studies indicated [16,18,44], dry-season productivity is lower than wet season productivity by approximately 27 per cent under the midday condition, which supports that a large part of Amazonia is water stressed during the dry season. This does not contradict the observed high evapotranspiration rate during the dry season because higher VPD and temperature during the dry season lower the water-use efficiency of photosynthesis [20,21]. We postulate that midday GPP decreases during the dry season because stomatal conductance decreases when hydraulic capacity cannot meet transpirational demand, particularly with increasing atmospheric VPD [21].

The balance between radiation and water stress is explored in more detail with SCOPE model simulations. Under low-light conditions, GPP increases linearly with increasing light intensity, but the increase saturates when photon flux density (PFD) is greater than approximately 400 μmol m^{-2} s^{-1} (figure 5). Given that Amazonian forests receive more than 400 μmol m^{-2} s^{-1} during the midday even in the wet season (see the electronic supplementary material, figure S3), water stress (higher VPD) leads to decreased GPP and as a result, GPP is lower during the dry season than the wet season. We note that during the dry season plants may maintain their chlorophyll content (e.g. greenness) but photosynthesize less owing to stomatal closure (except in the early morning when soil water potentials have had time to recover).

The regulation of stomatal aperture in response to variations in light intensity and VPD effectively operates as a mechanism to avoid hydraulic failure while maximizing GPP for a given amount of water loss [45]. Reduction in stomatal conductance with increasing VPD occurs even in mildly stressed vegetation. Partial closing of the stomata causes a temporal imbalance between carboxylation and light harvest owing to reduced diffusion of carbon dioxide into the mesophyll. The balance between carboxylation and light harvest is restored by reducing GPP and fluorescence [25].

Greenness indices are often used as proxies to estimate plant productivity [35,46]. However, it is known that greenness indices are difficult to interpret over Amazonia for many reasons: saturation over densely forested regions, varying treatments of atmospheric contamination of the MODIS optical bands [5], structural changes of forest canopy [7], and potential variations in the reflectance properties as leaves age [47]. MODIS LAI retrievals show opposite seasonality to fluorescence and EVI, peaking in the dry season, as opposed to fluorescence and EVI, which peak in the wet season (figure 2; [6]). Land Surface Models (e.g. National Center for Atmospheric Research Community Land Model)

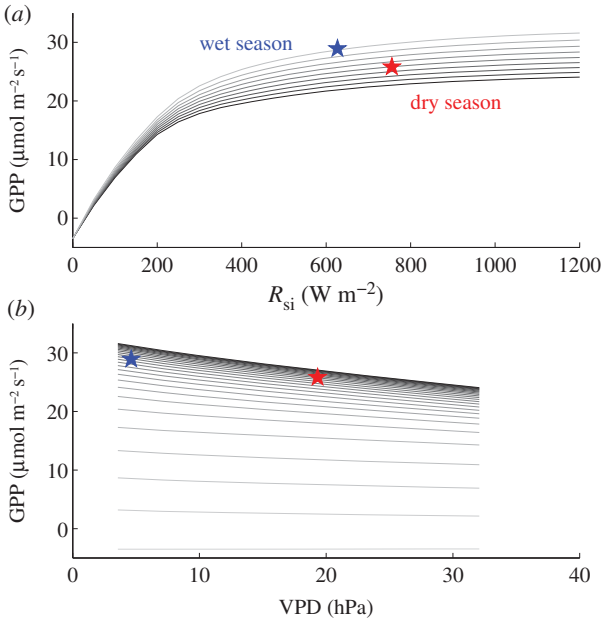

Figure 5. SCOPE-simulated relationships (*a*) between incoming radiation (R_{si}) and GPP and (*b*) between VPD and GPP. Different lines in (*a*) represent GPP values at different VPD ranging from 3.5 to 32 hPa in nearly equal steps (actual values are for relative humidity from 10 to 90%; high VPD values give low GPP values), and different lines in (*b*) represent GPP values at different solar energy from 50 to 1200 W m^{-2} in 50 W m^{-2} range (low solar radiation values give low GPP values). Midday incident radiation over Amazonia ranges between 400 and 800 W m^{-2} and VPD range from 3 to 40 hPa (see the electronic supplementary material, figure S3). The symbols indicate the mean midday ECMWF ERA values of VPD and irradiance during the dry (June-July-August) and wet (December-January-February) seasons of 2009 and 2010. (Online version in colour.)

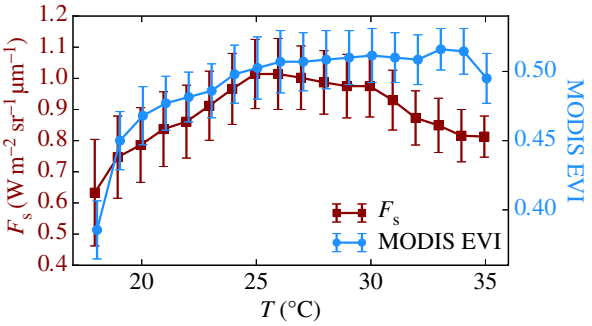

Figure 6. The relationship between temperature and fluorescence or EVI. Values are obtained over broadleaf evergreen trees between 20°S and 20°N, and error bars represent standard deviation. Temperature values are from ERA-Interim. Squares, F_s; circles, MODIS EVI. (Online version in colour.)

often use MODIS LAI [46], which causes these MODIS-based models to estimate higher productivity in the dry season than the wet season (opposite to fluorescence, electronic supplementary material, figure S4). Ground-based measurements over temperate evergreen forests also show that the maximum in LAI does not coincide with the maximum GPP: over the Metolius site in Oregon, United States, GPP maximum occurs in May or June, whereas LAI maximum occurs in August [48].

EVI is well-correlated with fluorescence ($r^2 = 0.52$) probably because both are sensitive to the absorbed PPFD, but diverges from fluorescence at the peak of the dry season, when EVI is greatest but fluorescence lowest (figure 2 and table 1). Moreover, for temperatures greater than 30°C, EVI does not change, whereas fluorescence decreases (figure 6). Also, EVI does not vary with VPD nor SCOPE GPP (figure 3*b*). Although EVI may be indicative of chlorophyll content (photosynthetic capacity), our analysis suggests that additional environmental conditions are necessary to determine GPP.

We conclude that measurements of sun-induced fluorescence provide new insight into the effect of drought on productivity in Amazonian forests. Still, the cumulative seasonal difference in GPP may not correspond exactly to that indicated by the midday clear-sky 'snapshots' provided by fluorescence because the cumulative radiation input may vary between seasons [5]. Anyway, GPP estimates from the Max Planck Institute for Biogeochemistry [49], a model that links GPP to water-use efficiency, shows similar seasonality to fluorescence (see the electronic supplementary material, figure S4).

Our results suggest that during severe dry conditions, such as in 2010, the Amazonian uptake of carbon from the atmosphere can decrease significantly because of the suppression of photosynthesis. Midday GPP is reduced by 15 per cent during the dry season (June to September) in 2010 compared with 2009. This decrease corresponds to a total GPP decrease of 0.8 P_gC when we use the linear relationship between GPP and fluorescence from [30]. GPP estimates from MODIS also show a 12 per cent reduction, strengthening the finding that fluorescence and greenness correspond better under more severe conditions. Fluorescence decreases over region A during 2010 drought owing to high water stress with precipitation less than 100 mm month^{-1}.

6. Summary and conclusion

Photosynthetic plant carbon assimilation is regulated by water availability and dynamic stomatal response. Our results indicate a strong synchronization of the carbon and water cycle over Amazonia [8] even under only moderate water stress levels through changes in vapour pressure deficit. Our results suggest that during severe dry conditions such as in 2010, Amazonian carbon uptake of carbon from the atmosphere can decrease significantly because of the larger suppression of photosynthesis during the dry season than the wet season (figure 2). Over the everwet area (region A), water stress is generally not high enough to influence fluorescence, but fluorescence (and GPP) decreases when precipitation falls below 100 mm month^{-1}.

While traditional greenness indices only capture the changes in reflectance owing to leaf loss or chlorophyll content—thus requiring ancillary meteorology data to estimate GPP [35]—fluorescence can capture the decreased GPP directly through radiative emission by the photosynthetic machinery as gas exchange lags with stomatal closure owing to mild water stress. Satellite measurements of fluorescence are sensitive to stomatal conductance as well as changes in chlorophyll content and hence, compared with vegetation indices, offer a more direct and complementary proxy for GPP over large scales. These data can be used to improve the representation of GPP in land surface models and to quantify the response of GPP to environmental stress. Satellite-based chlorophyll fluorescence opens a new approach to estimate photosynthetic rates of vegetation over large scales and to evaluate the impact of environmental parameters on GPP.

We acknowledge the entire GOSAT team for having designed and built the instrument and especially A. Kuze and H. Suto for their tremendous efforts in helping understand GOSAT calibration in the O2 A-band. We acknowledge all MODIS land product science team members for providing an invaluable public dataset. ECMWF ERA-Interim data used in this study have been provided by ECMWF. We thank M. Zhao (University of Montana) for providing the updated LAI and GPP products and M. Jung and M. Reichstein for providing the MPI-BGC dataset. We also thank anonymous reviewers and S. Saleska for providing careful and constructive comments on our manuscript. L.G.'s work has been funded by the Emmy Noether Programme of the German Research Foundation (GlobFluo project), and S.S. acknowledges the support by Carbon Cycle funding from NASA under terrestrial ecology. This research was carried out at the Jet Propulsion Laboratory, California Institute of Technology, under a contract with the National Aeronautics and Space Administration, and is supported in part by the W.M. Keck Institute for Space Studies.

References

1. Morley RJ. 2002 *Origin and evolution of tropical rain forests*. Chichester, UK: John Wiley.
2. Saatchi SS *et al*. 2011 Benchmark map of forest carbon stocks in tropical regions across three continents. *Proc. Natl Acad. Sci. USA* **108**, 9899–9904. (doi:10.1073/pnas.1019576108)
3. Dirzo R, Raven PH. 2003 Global state of biodiversity and loss. *Annu. Rev. Environ. Resour.* **28**, 137. (doi:10.1146/annurev.energy.28.050302.105532)
4. Saleska SR, Didan K, Huete AR, da Rocha HR. 2007 Amazon forests green-up during 2005 drought. *Science* **318**, 612. (doi:10.1126/science.1146663)
5. Samanta A, Ganguly S, Hashimoto H, Devadiga S, Vermote E, Knyazikhin Y, Nemani RR, Myneni RB. 2010 Amazon forests did not green-up during 2005 drought. *Geophys. Res. Lett.* **37**, 1–5. (doi:10.1029/2009GL042154)
6. Myneni RB *et al*. 2007 Large seasonal swings in leaf area of Amazon rainforests. *Proc. Natl Acad. Sci. USA* **104**, 4820–4823. (doi:10.1073/pnas.0611338104)
7. Anderson LO, Malhi Y, Aragao LEOC, Ladle R, Arai E, Barbier N, Phillips O. 2010 Remote sensing detection of droughts in Amazonian forest canopies. *New Phytol.* **187**, 733–750. (doi:10.1111/j.1469-8137.2010.03355.x)
8. Phillips OL *et al*. 2009 Drought sensitivity of the Amazon rainforest. *Science* **323**, 1344–1347. (doi:10.1126/science.1164033)
9. Li W, Fu R, Juarez RIN, Fernandes K. 2008 Observed change of the standardized precipitation index, its potential cause and implications to future climate change in the Amazon region. *Phil. Trans. R. Soc. B* **363**, 1767–1772. (doi:10.1098/rstb.2007.0022)
10. Lee J-E, Lintner BR, Boyce CK, Lawrence PJ. 2011 Land use change exacerbates tropical South American drought by sea surface temperature variability. *Geophys. Res. Lett.* **38**, L19706.
11. Mechl GA *et al*. 2007 Global climate projections. In *Climate Change 2007: the physical science basis.* Contribution of Working Group I to the fourth assessment report of the intergovernmental panel on climate change (eds S Solomon, D Qin, M Manning, Z Chen, M Marquis, KB Averyt, M Tignor, HL Miller), pp. 996. New York, NY: Cambridge University Press.
12. Li W, Fu R, Dickinson RE. 2006 Rainfall and its seasonality over the Amazon in the 21st century as assessed by the coupled models for the IPCC AR4. *J. Geophys. Res.* **111**, D02111. (doi:10.1029/2005JD006355)
13. Malhi Y, Aragao LEOC, Galbraith D, Huntingford C, Fisher R, Zelazowski P, Sitch S, McSweeney C, Mei P. 2009 Exploring the likelihood and mechanism of a climate-change-induced dieback of the Amazon rainforest. *Proc. Natl Acad. Sci. USA* **106**, 20 610–20 615. (doi:10.1073/pnas.0804619106)
14. Fisher JB *et al*. 2009 The land–atmosphere water flux in the tropics. *Glob. Change Biol.* **15**, 2694–2714. (doi:10.1111/j.1365-2486.2008.01813.x)
15. Nepstad *et al*. 1994 The role of deep roots in the hydrological and carbon cycles of Amazonian forests and pastures. *Nature* **372**, 666–669. (doi:10.1038/372666a0)
16. Lee J-E, Oliveira RS, Dawson TE, Fung I. 2005 Root functioning modifies seasonal climate. *Proc. Natl Acad. Sci. USA* **102**, 17 576–17 581. (doi:10.1073/pnas.0508785102)
17. Huete AR, Restrepo-Coupe N, Ratana P, Didan K, Saleska SR, Ichii K, Panuthai S, Gamo M. 2008 Multiple site tower flux and remote sensing comparisons of tropical forest dynamics in Monsoon Asia. *Agric. Forest Meteorol.* **148**, 748–760. (doi:10.1016/j.agrformet.2008.01.012)
18. Saleska SR *et al*. 2003 Carbon in Amazon forests: unexpected seasonal fluxes and disturbance-induced losses. *Science* **302**, 1554–1557. (doi:10.1126/science.1091165)
19. Goulden ML, Miller SD, da Rocha HR, Menton MC, Freitas HC, Figueira AMS, de Sousa CAD. 2004 Diel and seasonal patterns of tropical forest CO_2 exchange. *Ecol. Appl.* **14**, S42–S54. (doi:10.1890/02-6008)
20. Reichstein M *et al*. 2002 Severe drought effects on ecosystem CO_2 and H_2O fluxes at three Mediterranean evergreen sites: revision of current hypotheses? *Glob. Change Biol.* **8**, 999–1017. (doi:10.1046/j.1365-2486.2002.00530.x)
21. Lee J-E, Boyce CK. 2010 The impact of hydraulic capacity on water and carbon cycles in tropical South America. *J. Geophys. Res.* **115**, D23123. (doi:10.1029/2010JD014568)
22. Huete AR, Didan K, Shimabukuro YE, Ratana P, Saleska SR, Hutyra LR, Yang W, Nemani RR, Myneni R. 2006 Amazon forests green-up with sunlight in dry season. *Geophys. Res. Lett.* **33**, L06405. (doi:10.1029/2005GL025583)
23. Nepstad DC *et al*. 2002 The effects of partial throughfall exclusion on canopy processes, aboveground production, and biogeochemistry of an Amazon forest. *J. Geophys. Res.* **107**, D8085. (doi:10.1029/2001JD000360)
24. Asner GP, Alencar A. 2010 Drought impacts on the Amazon forest: the remote sensing perspective. *New Phytol.* **187**, 569. (doi:10.1111/j.1469-8137.2010.03310.x)
25. van der Tol C, Verhoef W, Rosema A. 2009 A model for chlorophyll fluorescence and photosynthesis at leaf scale. *Agric. Forest Meteorol.* **149**, 96–105. (doi:10.1016/j.agrformet.2008.07.007)
26. Flexas J, Flexas J, Escalona JM, Evain S, Gulias J, Moya I, Osmond CB, Medrano H. 2002 Steady-state chlorophyll fluorescence (*Fs*) measurements as a tool to follow variations of net CO_2 assimilation and stomatal conductance during water-stress in C3 plants. *Physiol. Plant.* **114**, 231–240. (doi:10.1034/j.1399-3054.2002.1140209.x)
27. Daumard F, Champagne S, Fournier A, Goulas Y, Ounis A, Hanocq J-F, Moya I. 2010 A field platform for continuous measurement of canopy fluorescence. *IEEE Trans. Geosci. Remote* **48**, 3358–3368. (doi:10.1109/TGRS.2010.2046420)
28. Galmés J, Medrano H, Flexas J. 2007 Photosynthetic limitations in response to water stress and recovery in Mediterranean plants with different growth forms. *New Phytol.* **175**, 81–93. (doi:10.1111/j.1469-8137.2007.02087.x)
29. Frankenberg C, Butz A, Toon GC. 2011 Disentangling chlorophyll fluorescence from atmospheric scattering effects in O_2A-band spectra of reflected sun-light. *Geophys. Res. Lett.* **38**, L03801.
30. Frankenberg C *et al*. 2011 New global observations of the terrestrial carbon cycle from GOSAT: patterns of plant fluorescence with gross primary productivity. *Geophys. Res. Lett.* **38**, L17706.
31. Meroni M, Rossini M, Guanter L, Alonso L, Rascher U, Colombo R, Moreno J. 2009 Remote sensing of solar-induced chlorophyll fluorescence: review of methods and applications. *Remote Sens. Environ.* **113**, 2037–2051. (doi:10.1016/j.rse.2009.05.003)
32. Moya I, Ounis A, Moise N, Goulas Y. 2006 First airborne multiwavelength passive chlorophyll fluorescence measurements over La Mancha (Spain) fields. In *Second recent advances in quantitative remote sensing* (ed. JA Sobrino), pp. 820. Spain: Publicacions de la Universitat de València.
33. Joiner JY, Yoshida Y, Vasilkov AP, Yoshida Y, Corp LA, Middleton EM. 2011 First observations of global and seasonal terrestrial chlorophyll fluorescence from space. *Biogeosciences* **8**, 637–651. (doi:10.5194/bg-8-637-2011)

34. Frolking S, Milliman T, Palace M, Wisser D, Lammers R, Fahnestock M. 2011 Tropical forest backscatter anomaly evident in SeaWinds scatterometer morning overpass data during 2005 drought in Amazonia. *Remote Sens. Environ.* **115**, 897–907. (doi:10.1016/j.rse.2010.11.017)
35. Zhao M, Running SW. 2010 Drought-induced reduction in global terrestrial net primary production from 2000 through 2009. *Science* **329**, 940–943. (doi:10.1126/science.1192666)
36. Frankenberg C, O'Dell C, Guanter L, McDue J. 2012 Remote sensing of near-infrared chlorophyll fluorescence from space in scattering atmospheres: implications for its retrieval and interferences with atmospheric CO_2 retrievals. *Meas. Tech.* **5**, 2081–2094. (doi:10.5194/amt-5-2081-2012)
37. Saatchi SS, Asefi-Najafabady S, Malhi Y, Aragao LEOC, Anderson LO, Myneni RB, Nemani R. 2013 Persistent effects of a severe drought on Amazonian forest canopy. *Proc. Natl Acad. Sci. USA* **110**, 565–570. (doi:10.1073/pnas.1204651110)
38. van der Tol C, Verhoef W, Timmermans J, Verhoef A, Su Z. 2009 An integrated model of soil-canopy spectral radiances, photosynthesis, fluorescence, temperature and energy balance. *Biogeosciences.* **6**, 3109–3129. (doi:10.5194/bg-6-3109-2009)
39. Farquhar G, Von Caemmerer S, Berry J. 1980 A biochemical model of photosynthetic CO_2 assimilation in leaves of C3 species. *Planta* **149**, 78–90. (doi:10.1007/BF00386231)
40. Collatz G, Ribas-Carbo M, Berry JA. 1992 Coupled photosynthesis-stomatal conductance model for leaves of C4 plants. *Aus. J. Plant Physiol.* **19**, 519–538. (doi:10.1071/PP9920519)
41. Miller J *et al*. 2005 Development of a vegetation fluorescence canopy model. ESTEC contract no. 16365/02/NL/FF, final report.
42. Baker N. 2008 Chlorophyll fluorescence: a probe of photosynthesis *in vivo*. *Ann. Rev. Plant Biol.* **59**, 89–113. (doi:10.1146/annurev.arplant.59.032607.092759)
43. Duysens LMN, Sweers HE. 1963 Mechanism of two photchemical reactions in algae as studied by means of fluorescence. In *Studies on microalgae and photosynthetic bacteria,* special issue of plant and cell physiology (ed. E Ashida), pp. 353–372. Tokyo, Japan: University of Tokyo Press.
44. Oliveira R, Dawson TE, Burgess S, Nepstad D. 2005 Hydraulic redistribution in three Amazonian trees. *Oecologia* **145**, 354–363. (doi:10.1007/s0042-005-0108-2)
45. Cowan I, Farquhar G. 1977 Stomatal function in relation to leaf metabolism and environment. *Soc. Exp. Biol. Symp.* **31**, 471–505.
46. Lawrence PJ, Chase TN. 2007 Representing a new MODIS consistent land surface in the Community Land Model (CLM 3.0). *J. Geophys. Res.* **112**, G01023. (doi:10.1029/2006JG000168)
47. Brando PM, Goetz SJ, Baccini A, Nepstad DC, Beck PSA, Christman MC. 2010 Seasonal and interannual variability of climate and vegetation indices across the Amazon. *Proc. Natl Acad. Sci. USA* **107**, 14 685–14 690. (doi:10.1073/pnas.0908741107)
48. Law B, Williams M, Anthoni P, Baldocchi D, Unsworth M. 2000 Measuring and modelling seasonal variation of carbon dioxide and water vapour exchange of a pinus ponderosa forest subject to soil water deficit. *Glob. Change Biol.* **6**, 613–630. (doi:10.1046/j.1365-2486.2000.00339.x)
49. Beer C *et al*. 2010 Terrestrial gross carbon dioxide uptake: Global distribution and covariation with climate. *Science* **329**, 834–838. (doi:10.1126/science.1184984)